JOURNAL OF CATALYSIS 140, 575–584 (1993)

The Effect of Coadsorbates in Reverse Water–Gas Shift Reaction on ZnO, in Relation to Reactant-Promoted Reaction Mechanism

TAKAFUMI SHIDO[1] AND YASUHIRO IWASAWA[2]

Department of Chemistry, Faculty of Science, the University of Tokyo, Hongo, Bunkyo-ku, Tokyo 113, Japan

Received July 23, 1992; revised October 20, 1992

A reactant-promoted reaction mechanism for reverse water–gas shift reaction ($H_2 + CO_2 \rightarrow H_2O + CO$; r-WGSR) on ZnO was investigated by FT-IR, MS, and GC. Surface bidentate formate was produced from $H_2 + CO_2$ through bidentate carbonate. The decomposition rate of the formate as a reaction intermediate became 1/10 ~ 1/30 of that in vacuum by the coexistence of CO_2. On the contrary, the decomposition rate of the formate was promoted 8–10 times by the coexistence of H_2 as compared with that in vacuum. The activation energy decreased from 171 kJ mol^{-1} in vacuum to 138 kJ mol^{-1} in H_2. About 70% of the surface formates decomposed to H_2 and CO_2 and about 30% of them decomposed to $H_2O(-OH)$ and CO. The decomposition selectivity of the surface formate was not changed by H_2. The decomposition selectivity was much different from that for the bidentate formate produced from $-OH(H_2O)$ and CO. It was suggested that WGSR and r-WGSR proceeded through bidentate formates, but at different sites on ZnO. The rate of r-WGSR was between the decomposition rates of the formates under CO_2 and H_2, indicating that the rate of r-WGSR is balanced with H_2 promotion and CO_2 suppression. The rate determining step is the dissociation of H_2 at the (Zn-formate–OH)pair site. The rate constant for the formate decomposition increased linearly with the amount of adsorbed H_2. H_2 molecules not only act as a reactant to reduce the bidentate carbonate to the bidentate formate, but also promote the decomposition of the bidentate formate to $H_2O(-OH) + CO$ or $H_2 + CO_2$.

INTRODUCTION

We have reported the reactant-promoted reaction mechanism for the catalytic water–gas shift reaction ($H_2O(-OH) + CO \rightarrow H_2 + CO_2$; WGSR) on MgO (*1*), ZnO (*2*), CeO_2 (*3*), and Rh/CeO_2 (*4*) as the genesis of catalysis. Water molecules readily dissociate on these oxide surfaces to form terminal and bridge OH groups. The terminal OH groups react with CO to produce surface formates like unidentate, bidentate, and bridge formates. While the surface formates have been believed to be reaction intermediates for WGSR, actually no or few surface formates are converted to the products, H_2 and CO_2, by themselves in vacuum. For example, 70% of bidentate formates produced from $-OH + CO$ on ZnO decompose backwardly to $-OH$ and CO and only 30% of them decompose forwardly to H_2 and CO_2 in vacuum. On the contrary, almost 100% of the formate decompose to $H_2 + CO_2$ in the coexistence of water. In the reactant-promoted mechanism the forward decomposition rate is promoted by the reactant molecules and the activation energy also decreases. This phenomenon corresponds to the creation of a new reaction path in catalytic reaction conditions different from a stoichiometric (noncatalytic) reaction.

WGSR is an equilibrium reaction, and the reverse water gas–shift reaction ($H_2 + CO_2 \rightarrow H_2O + CO$; r-WGSR) also proceeds on the ZnO surface (*5*, *6*). It is interesting to investigate whether there is or is not the reactant-promoted mechanism involving activation of intermediates in r-WGSR. As

[1] Present address: Catalysis Research Center, Hokkaido University, Sapporo 060, Japan.

[2] To whom correspondence should be addressed.

0021-9517/93 $5.00

surface formates produced from H_2 and CO_2 are believed to be reaction intermediates in r-WGSR (*5*), we have investigated the behavior of surface formates in the elementary reaction steps and the catalytic reaction in this article. Surface formates on ZnO were produced by two ways, from $-OH + CO$ and $H_2 + CO_2$. The behaviors of these formates were also compared to examine the nature of the intermediate of an equilibrium reaction.

EXPERIMENTAL

Experimental conditions are described in the previous paper (*2*). Briefly, 25 mg of ZnO powder (Kadox-15) was pressed into a self-supporting wafer and set into an IR cell. The ZnO wafer was oxidized with O_2 at 773 K followed by evacuation at the same temperature. To replace surface OH groups by OD groups, the sample was exposed to D_2O at 473 K followed by evacuation at 773 K. IR spectra were measured at room temperature or in reaction conditions with a resolution of 2 or 4 cm^{-1} on a JEOL JIR-10 FT-IR spectrometer. To measure TPD spectra or reaction rates at given (fixed) temperatures, 0.2 g of ZnO powder was set into a U-shaped Pyrex-glass reactor that was combined with a closed circulating system (base pressure was 1×10^{-4} Pa). The desorbed products were analyzed by mass spectrometry and gas chromatography. Catalytic r-WGSR was also conducted in a closed circulating system equipped with a mass spectrometer and a gas chromatograph.

RESULTS

Figure 1 shows IR spectra of the species produced by exposure of the ZnO surface to D_2 and CO_2 at different temperatures. When the sample was exposed to CO_2 (4.0 kPa) and D_2 (4.0 kPa) at 323 K, IR bands appeared at 2667, 1579, 1513, 1425, 1341, and 1010 cm^{-1}. When the sample was exposed to $CO_2 + D_2$ at 423 K, the other bands at 2602, 2171, and 1568 cm^{-1} appeared. By increasing temperature for exposure, the intensity of the peaks at 2667, 1579, 1513, 1425, and 1010 cm^{-1} decreased and the intensity of the peaks at 2602, 2171, and 1568 cm^{-1} increased.

Table 1 summarizes IR bands observed on ZnO surface by exposure to a mixture of hydrogen (deuterium) and CO_2. The assignment of species is discussed hereinafter. IR bands at 2171, 1568 and 1342 cm^{-1} are attributed to ν(CD), ν_{as}(OCO), and ν_s(OCO)

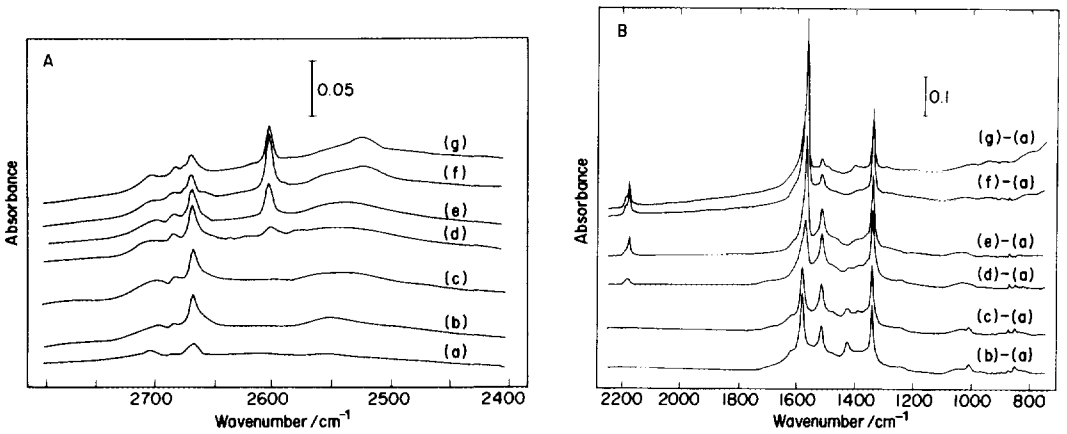

FIG. 1. IR spectra in two frequency regions ((A) and (B)) of surface species produced by exposure of ZnO preevacuated at 773 K (spectrum (a)) to D_2 (4.0 kPa) + CO_2 (4.0 kPa) at (b) 323 K, (c) 373 K, (d) 423 K, (e) 473 K, (f) 523 K, and (g) 573 K. In spectra (B), each spectrum was subtracted by the spectrum of ZnO itself (a).

TABLE 1

IR Bands of Adsorbate on ZnO

Species	Absorption bands/cm^{-1}[a]
Bidentate formate	ν(CH), 2875; ν_{as}(OCO), 1572; ν_s(OCO), 1371 (2170) (1568) (1342)
Bidentate carbonate	ν(C=O), 1579; ν_{as}(OCO), 1341; ν_s(OCO), 1010
Unidentate carbonate	ν_{as}(OCO), 1425
Carboxylate	ν_{as}(OCO), 1513; ν_s(OCO), 1341 (tentative)

[a] The values in parentheses are the ones for DCOO(ad).

of bidentate formate, respectively, which are almost the same frequencies as those for bidentate formate previously reported (*2*). The IR bands at 1579, 1341 and 1010 are assignable to ν(C=O), ν_{as}(OCO), and ν_s(OCO) of bidentate carbonate, respectively. The peaks at 2667 and 2601 cm^{-1} are due to surface OD groups which are produced by contacting ZnO surface with D_2.

Figure 2 shows IR spectra of surface species produced by exposure of ZnO to D_2 + CO_2 at 523 K, followed by evacuation at different temperatures. The intensity of the IR bands at 2171, 1568, and 1342 cm^{-1} decreased by evacuation at 573 K and disappeared at 623 K. Similarly, the intensity of the IR band at 2602 cm^{-1} decreased by evacuation at 573 K and disappeared at 623 K. The surface formates and the OD groups produced by CO_2 + D_2 were observed to behave in a similar way upon heating in Fig. 2. Both of them were produced at 423 K in Fig. 1 and decomposed at 573 K in Fig. 2.

Figure 3 shows TPD spectra of surface formates produced by H_2 (4.0 kPa) + CO_2 (4.0 kPa). The sample was exposed to a mixture of H_2 + CO_2 at 523 K followed by evacuation (base pressure: 1.3×10^{-3} Pa) at 473 K for 4.5 h. Then the temperature was linearly increased at a heating rate of 4 K min^{-1}. The pressure of the system during TPD measurement was less than 5 Pa. The desorbed products were taken for mass spectroscopic analysis at an appropriate interval, followed by 2 s evacuation of the system to remove the remaining gas phase sample. Under these conditions the H_2 and CO_2 products have no effect on the rate of decomposition. About one tenth of the desorbed species was taken for the analysis. Desorption peaks of H_2, CO_2, and CO appeared at 550, 590, and 580 K with the desorption amounts of 9.2, 10.2, and 2.6 μmol g_{cat}^{-1}, respectively. The desorption amounts of H_2 and CO_2 are similar to each other, which are ca. four times as large as that of CO. Almost no water desorbed during TPD, because produced water may be trapped on the ZnO surface as surface OH.

Figures 4 and 5 show Arrhenius plots for the decomposition of surface formates from D_2 + CO_2 and that from −OD + CO, respectively. The total decomposition rate was calculated from the decrease in the intensity of the IR band (simple absorbance of ν(CD)) for DCOO at given (fixed) temperatures. The rate of forward decomposition (DCOO + (D) → D_2O + CO; k_+) and that of backward decomposition (DCOO + (D) → D_2 + CO_2; k_-) were calculated from the produced amounts of CO and D_2, respectively, at given (fixed) temperatures by means of MS spectrometer. The surface formate from D_2 + CO_2 was formed in a similar way to that in the TPD experiment in Fig. 3, and the formate from −OD + CO was formed in a similar way to that described in the previous paper (*2*).

The decomposition rate of surface formate (from D_2 + CO_2) under 4.0 kPa of CO_2 decreased to 1/10 of that in vacuum as

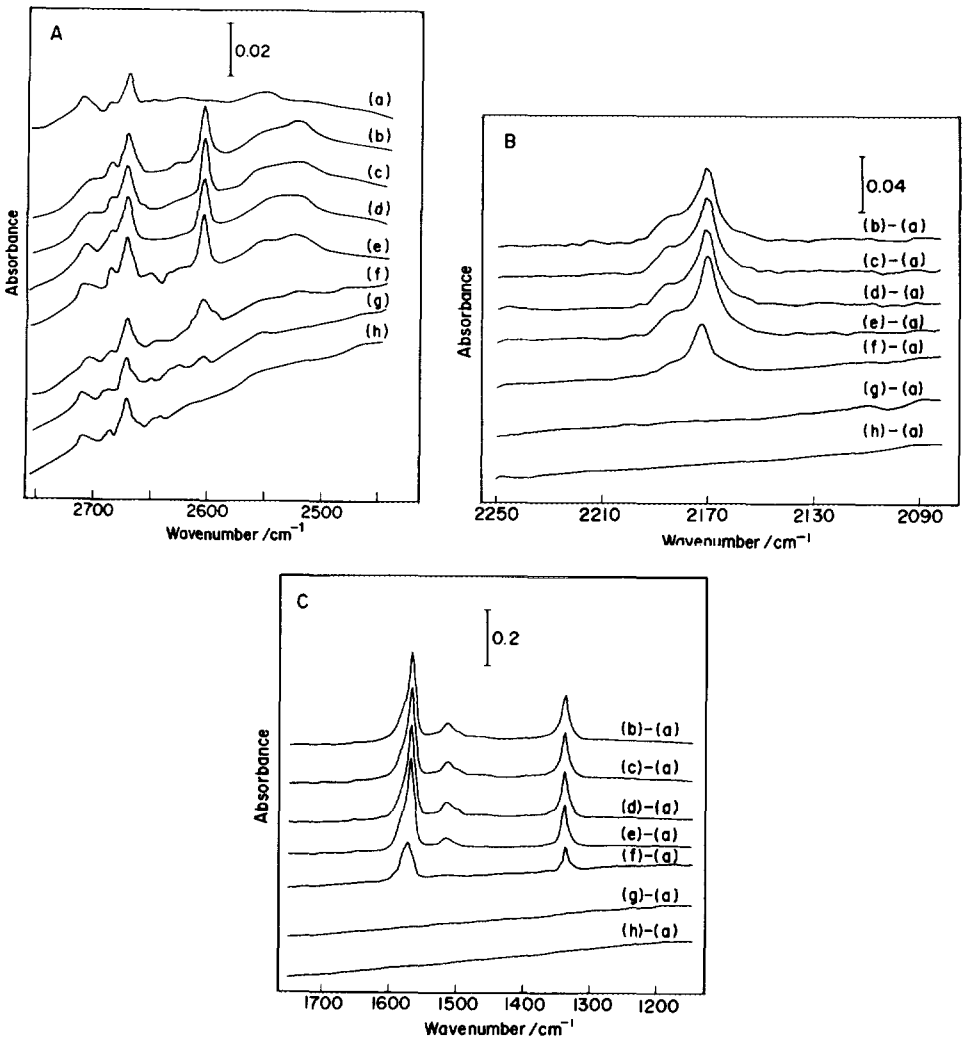

FIG. 2. IR spectra in three frequency regions ((A), (B), and (C)) of surface species on ZnO (pre-evacuated at 773 K; spectrum (a)) produced by $D_2 + CO_2$. The sample was exposed to $D_2 + CO_2$ at 523 K followed by evacuation at (b) 373 K, (c) 423 K, (d) 473 K, (e) 523 K, (f) 573 K, (g) 623 K, and (h) 673 K. In spectra (B) and (C), each spectrum was subtracted by the spectrum of ZnO itself (a).

shown in Fig. 4. On the other hand, the decomposition rate in 4.0 kPa of H_2 increased in Fig. 4. The activation energies for the formate decomposition (total) in vacuum, under H_2, and under CO_2 were obtained to be 171, 138, and 244 kJ mol^{-1}, respectively.

The activation energies for the decomposition of the formate (from $-OD + CO$) in vacuum, under H_2 (4.0 kPa), and under CO_2 (4.0 kPa) were determined to be 155, 120, and 242 kJ mol^{-1}, respectively. Decomposition selectivity for the formates produced from $-OH + CO$ and $H_2 + CO_2$ was different each other. Seventy percent of the formates from $-OH + CO$ decomposed to $-OH + CO$ and 30% of them decomposed to $H_2 + CO_2$. On the contrary, 30% of the formates from $H_2 + CO_2$ decomposed to $-OH(H_2O) + CO$ and 70% of them decom-

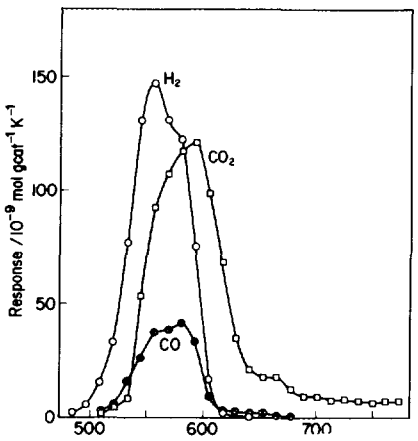

FIG. 3. TPD spectra of surface formate produced by H_2 + CO_2 on ZnO. The sample was exposed to H_2 + CO_2 at 523 K, followed by evacuation at 473 K for 4.5 h; Heating rate: 4.0 K min^{-1}.

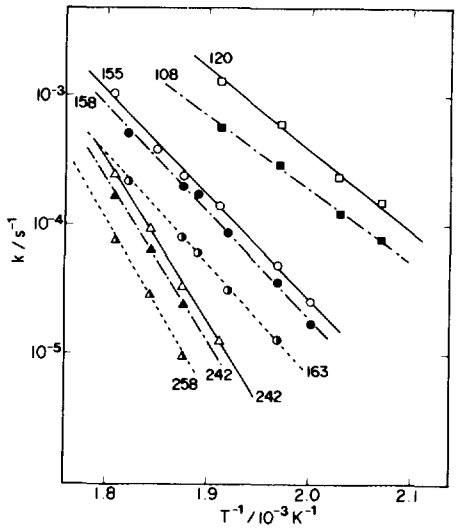

FIG. 5. Arrhenius plots of the decomposition of DCOO produced from OD + CO on ZnO. (○)k_+ + k_-, (●)k_+, and (○)k_- under vacuum; (□)k_+ + k_- and (■)k_+ in H_2 (4.0 kPa); (△)k_+ + k_-, (▲)k_+, and (△)k_- in CO_2 (4.0 kPa). The arabic numbers are the activation energies (kJ mol^{-1}). Definitions of k_+ + k_-, k_+, and k_- are described in the legend of Fig. 4.

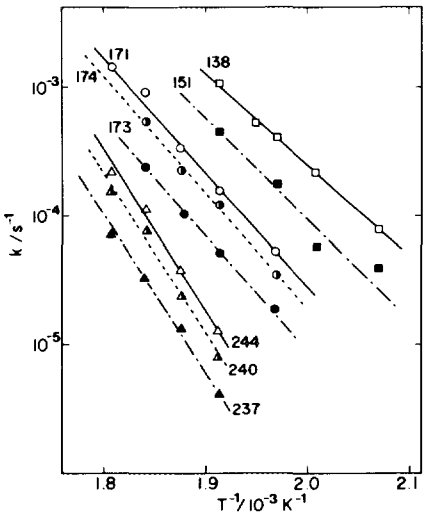

FIG. 4. Arrhenius plots for the decomposition of DCOO produced from D_2 + CO_2 on ZnO. Total rate constants (k_- + k_-) were calculated from IR spectra and the rate constants k_+ and k_- for the decomposition to H_2O (−OH) + CO and H_2 + CO_2, respectively, were measured by MS spectrometer. (○)k_+ + k_-, (●)k_+, and (○)k_- under vacuum; (□)k_+ + k_- and (■)k_- in H_2 (4.0 kPa); (△)k_+ + k_-, (▲)k_+, and (△)k_- in CO_2 (4.0 kPa). The arabic numbers are the activation energies (kJ mol^{-1}).

posed to H_2 + CO_2. Decomposition selectivity of the both formates was not changed by the coexistence of H_2 or CO_2.

Figure 6 shows the intensity of ν(CD) (2171 cm^{-1}) of the formate produced from D_2 + CO_2 as a function of reaction time at

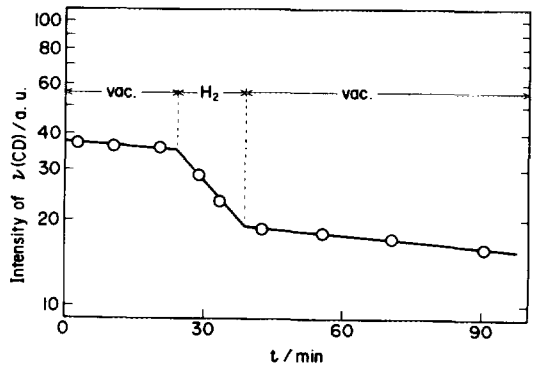

FIG. 6. Intensity of ν(CD) of the formate produced from D_2 + CO_2 as a function of reaction time at 508 K in vacuum and H_2.

508 K in vacuum and in H_2. In the initial stage of the formate decomposition in vacuum until 25 min, the rate constant ($k_+ + k_-$) was 5.3×10^{-5} s^{-1}. In the period from 25 min to 35 min under hydrogen, the rate constant increased to 4.1×10^{-4} s^{-1}. After 35 min in vacuum again the rate constant was as small as 5.3×10^{-5} s^{-1} as before. The rate was promoted ca. nine times by the coexistence of hydrogen. The phenomenon was reversible. Figure 7 shows the decomposition rate of the formate produced from $D_2 + CO_2$ as a function of the amount of hydrogen adsorbed. The rate constant was determined from the initial rate of the decomposition in the presence of various amounts of adsorbed hydrogen. The amount of adsorbed hydrogen was measured volumetrically under the identical conditions, independently of the IR measurements. The rate constant of the decomposition increased linearly with an increase of the amount of hydrogen adsorbed.

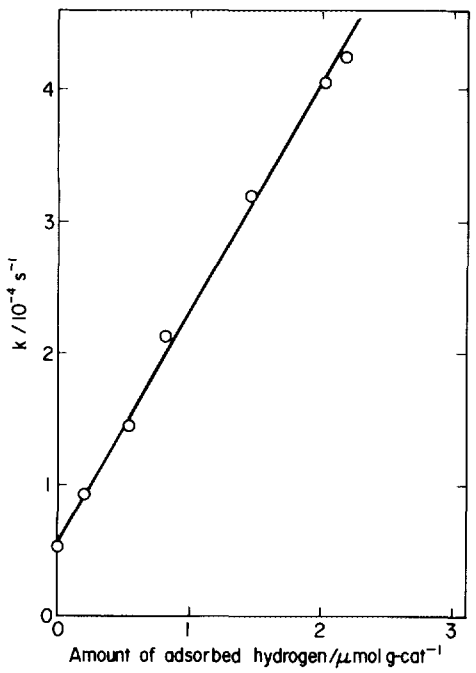

FIG. 7. Dependency of decomposition rate ($k_+ + k_-$) of the bidentate formate produced from $D_2 + CO_2$ at 508 K on the amount of adsorbed H_2.

TABLE 2

Rate Constants for the Decomposition of Formate in Various Combinations of Labeled Formate and Hydrogen[a]

Combination	$k_+ + k_-/10^{-4}$ s^{-1}
$HCOO + H_2$	4.4
$HCOO + D_2$	2.1
$DCOO + H_2$	4.1
$DCOO + D_2$	2.0

[a] T = 508 K, $p(H_2)$ or $p(D_2)$ = 4.0 kPa.

Table 2 shows the rate constants for the decomposition of formates in various isotope combinations. The isotope of the hydrogen molecule had a profound effect on the decomposition rate. On the contrary, the rate was not affected by the hydrogen isotope of formate. It suggests that the rate-determining step of the decomposition is the dissociation of hydrogen molecules.

Table 3 compares the rate constants of the forward decomposition of the formate produced from $D_2 + CO_2$ to $-OD$ (D_2O) + CO and the rate constants (k_+ (calc)) calculated from the catalytic reaction rate of r-WGSR in various conditions. The calculated rate constants are intermediate values between that under hydrogen and that under CO_2.

DISCUSSION

1. Formation process of the formate from $CO_2 + H_2$ and comparison of the formate from $H_2 + CO_2$ with that from ($-OH$ + CO). The IR bands at 1579, 1513, 1425, 1341, and 1010 cm^{-1} in Fig. 1 are not assigned to surface formates because ν(CD) band is not observed. Bidentate carbonates on oxide surfaces have three IR bands around 1600, 1280, and 1030 cm^{-1} attributed to ν(C=O), ν_{as}(OCO) and ν_s(OCO), respectively (*7*). Saussey *et al.* measured IR spectra of adsorbed CO_2 on ZnO (*8*) and observed several kinds of bidentate carbonates which show the IR bands at {1595, 1339, 1000, 848, and 680 cm^{-1}}, {1615, 1346, 999, 841, and 677

TABLE 3

Comparison of the Observed Rate Constant for the Decomposition of Bidentate Formate (DCOO) with the Calculated Value from the Reaction Rate of r-WGSR

T/K	Rate[a]	M[b]	k_- (calc)[c]	k_- (vac)[d]	k_+ (H_2)[e]	k_- (CO_2)[f]
493	1.67	5.5	3.0	1.6	12	0.06
508	4.83	5.2	9.3	3.8	33	0.26
523	10.33	5.7	18.1	11.9	90	1.2

Note. In footnotes *c*, *d*, *e*, and *f*, k_+ is the rate constant for the decomposition of formate to D_2O (−OD) + CO.

[a] In 10^{-10} mol s^{-1} g^{-1}.

[b] Amount of adsorbed formate in reaction conditions, in μmol g_{cat}^{-1}.

[c] Rate constants calculated from the reaction rate of r-WGSR, in 10^{-5} s^{-1}.

[d] Rate constants *in vacuum*, *in* 10^{-5} s^{-1}.

[e] Rate constants under H_2, in 10^{-5} s^{-1}.

[f] Rate constants under CO_2, in 10^{-5} s^{-1}.

cm^{-1}}, {1580, 1348, 1007, and 852 cm^{-1}} and {1665 and 1303 cm^{-1}}. Thus, the bands at 1579, 1341 and 1010 cm^{-1} in Fig. 1 are assigned to ν(C=O), ν_{as}(OCO), and ν_s(OCO) of bidentate carbonate, respectively. In fact, no peak in ν(CD) region was observed in the spectra (b) and (c) in Fig. 1. The bands of 1579 and 1010 cm^{-1} behaved in a similar way upon heating in Fig. 1, suggesting the peaks derived from the same species. The peak at 1341 cm^{-1} happened to be almost the same in position as the peak at 1342 cm^{-1} for ν_s (OCO) of bidentate formate. The bands at 2171, 1568, and 1342 cm^{-1} are assigned to bidentate formate (*2*, *6*): Those frequencies are almost the same as 2170, 1568, and 1342 cm^{-1} for bidentate formate produced from −OD + CO (*2*). The ν(CD) peak of 2171 cm^{-1} shifted to 2875 cm^{-1} for ν(CH) by using H_2 instead of D_2 (Table 1). These three peaks diminished similarly with each other upon heating and disappeared at the same temperature as shown in Fig. 2.

It is known that hydrogen adsorbs on the ZnO surface reversibly at room temperature, showing the IR bands at 1712 cm^{-1} (ν(Zn–H)) and 3490 cm^{-1} (ν(O_L–H)) for H_2, and 1233 cm^{-1} (ν(Zn–D)) and 2584 cm^{-1} (ν(O_L–D)) for D_2, where O_L represents lattice oxygens of hollow sites (*10*, *11*). The IR band at 2602 cm^{-1} shown in Figs. 1 and 2 shifted to 3521 cm^{-1} when CO_2 + H_2 was admitted to the system. Thus the 2602-cm^{-1} peak is attributable to ν(O_L–D). This band was not observed in the previous report (*2*), where the D_2O-treated ZnO sample was evacuated at 673 K. The peak at 2602 cm^{-1} disappeared above 623 K as shown in Fig. 2, while the peak at 2667 cm^{-1} which is also assigned to ν(O_L–D) remained at 673 K, similar to the previous observation (*2*). Hydrogen (deuterium) forms relatively weaker O_L–H (O_L–D) bond (lower frequency) as compared with H_2O (D_2O): This may be caused by less electron density of O_L–H bond (*12–14*). When the ZnO sample was exposed to CO_2 + D_2 at 323 and 373 K, no Zn–D or O_L–D bands appeared. Only bidentate carbonate appeared. These results suggest that CO_2 adsorbs as bidentate carbonate to block hydrogen dissociation.

When the sample was exposed to CO_2 + D_2 above 423 K, the bidentate carbonate diminished, while the bands that correspond to bidentate formate and hollow site OD (O_L–D) appeared in Fig. 1. Zn–D was not observed. These results suggest that the formate is produced from bidentate carbonate and hydrogen and that hydrogen atoms are not located on Zn atoms.

Bidentate formates with ν(CH), ν_{as}(OCO), and ν_s(OCO) shown in Table 1

are formed from both $-OH(H_2O) + CO$ and $H_2 + CO_2$. However, the activation energy for the formate decomposition in vacuum was 155 kJ mol^{-1} or 171 kJ mol^{-1} for the formates produced from $-OH + CO$ or $H_2 + CO$, respectively, as shown in Figs. 4 and 5. The selectivities for the decomposition at 533 K were also different from each other as follows:

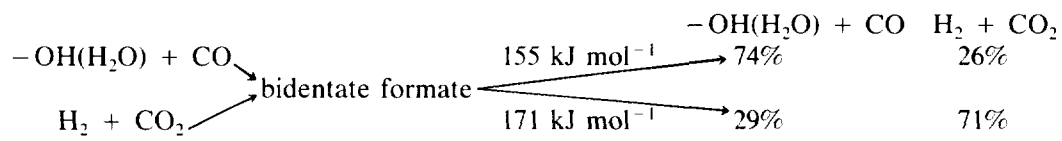

This drastic difference of selectivity is not clear at present, but it should not be ascribed to the difference of the bonding feature in Zn-formate species because of the same frequencies of ν(CH), ν_{as}(OCO), and ν_s(OCO) for both bidentate formates. Again, it should not be due to the difference in enthalpy for the species because the difference of two activation energies (155 and 171 kJ mol^{-1}) are not so large. Thus the selectivity of formate decomposition in vacuum may be entropically controlled, where the origin from which the formate was produced is remembered as a main reaction path.

2. Influence of coadsorbed species on the decomposition process of formates. As shown in Figs. 4, 5, and 6, the decomposition of surface formates was promoted 8–10 times by the coexistence of hydrogen. The activation energy for the decomposition also changed from 171 kJ mol^{-1} in vacuum to 138 kJ mol^{-1} in H_2 for the ($D_2 + CO_2$)-derived formate, or from 155 kJ mol^{-1} in vacuum to 120 kJ mol^{-1} in H_2 for the ($-OD + CO$)-derived formate. The possibility that reduction of ZnO surface by hydrogen causes the increase of decomposition rate can be ruled out because the decomposition rate increases only under hydrogen atmosphere and the decomposition rate decreases to the previous value immediately after evacuation of H_2, as shown in Fig. 6. Further, the increase in the initial rate (rate constant) of formate decomposition with the amount of adsorbed hydrogen in Fig. 7, together with the quick response of the reaction to the atmosphere in Fig. 6, may also exclude the possibility of the increase of rate by surface reduction. Again, the first-order rate constant for the decomposition was proportional to the adsorbed amount of hydrogen, which suggests that the adsorbed hydrogen directly interacts with surface formates to promote the decomposition.

Electron-donating molecules such as water, methanol, pyridine, and ammonia promoted the decomposition ($HCOO + H(a) \rightarrow H_2 + CO_2$) and suppressed the decomposition ($HCOO \rightarrow -OH + CO$) in WGSR (*2*). In r-WGSR hydrogen promotes both decompositions and the decomposition selectivity does not change. Thus the promotion way of hydrogen may be different from that of electron donors. The isotope effect of hydrogen on the rate constant was observed with the isotope of admitted hydrogen molecules, as shown in Table 2. This implies that the dissociation of hydrogen is a key step for the rate determination. Hydrogen dissociates heterolytically on ZnO surface to form $Zn–H^{\delta-}$ and $O–H^{\delta+}$ (*10, 11*). The hydrogen ($Zn–H^{\delta-}$) behaves as an electron donor to the bottom Zn ion. The mode of electron donor–acceptor interaction is different between hydrogen and the other molecules. Water, methanol, pyridine and ammonia interact with Zn ion by the lone pair electrons of the *p* orbital, whereas in the case of hydrogen the *s*-electron plays a role in electronic interaction. Thus the different interaction feature may cause the different promoting effects observed with hydrogen and the other donors.

CO_2 restrains the decomposition of for-

mates as shown in Table 3 and Figs. 4 and 5, while the selectivity of formate decomposition under CO_2 does not change. CO_2 not only blocks the adsorption sites of H_2 but also suppresses the decomposition itself. This stabilization of bidentate formate by the coexistence of CO_2 is a reverse phenomenon against that observed with the electron donors, suggesting the suppression of the decomposition by electron withdrawing effect of adsorbed CO_2. The peak at 1425 cm^{-1} assigned to unidentate carbonate appeared by exposing ZnO to D_2 + CO_2 at 323-373 K, but disappeared at 473 K as shown in Fig. 1, excluding the possibility of the suppression due to the unidentate carbonate. The carboxylate at 1513 cm^{-1} (ν_{as}(OCO)) still remained at reaction temperatures. The carboxylate coordinated to Zn ion might behave as an electron acceptor. The rate constant obtained from catalytic r-WGSR was larger than that in vacuum, suggesting the H_2 promotion in reaction conditions, but it was smaller than that for the formate decomposition in H_2, suggesting some restriction by CO_2. As a result, r-WGSR proceeds with a balance of the H_2 promotion and the CO_2 suppression.

3. Reaction mechanism of reverse WGSR including reactant-promoted effect. Decomposition of surface formate is influenced by coadsorbates during r-WGSR. Hydrogen promotes the decomposition of bidentate formate and CO_2 restrains the decomposition. As two reactants of r-WGSR interact with the formate in an opposite way, the calculated rate constants for the decomposition of the formate are intermediates as shown in Table 3.

Scheme 1 shows a reaction mechanism of r-WGSR on ZnO. Surface bidentate carbonates are produced from CO_2. Hydrogen reduces the bidentate carbonate to bidentate formate and hollow site OH. When the formate decomposed, the IR band of OH disappeared, as shown in Fig. 2: 70% of bidentate formate from CO_2 + H_2 decomposed to CO_2 + H_2 and 30% of them decomposed to CO + H_2O (−OH). CO_2 remarkably

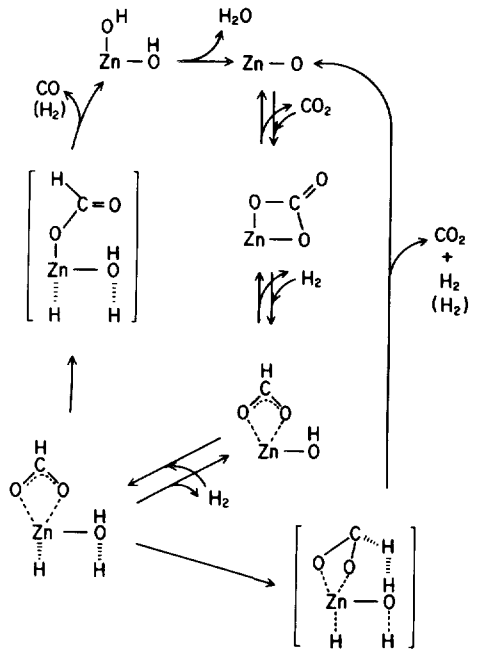

SCHEME 1. Reaction mechanism of reverse WGSR on ZnO.

suppresses the formate decomposition as shown in Table 3. Hence the bidentate formate stabilized by CO_2 (carbonate) does not positively contribute to the rate of the decomposition in r-WGSR conditions. In the mechanism of Scheme 1 the promotion by H_2 is only illustrated. The facts that H_2 promotes the decomposition of bidentate formate and that the rate constant linearly increased with adsorbed amount of H_2 indicate the presence of the (Zn-bidentate formate–OH) pair site at which H_2 absorbs in r-WGSR. The hydrogen isotope effect suggests that the rate-determining step is the dissociation of H_2 at the pair site. The bidentate formate may be decomposed to CO + −OH(H_2O) through unidentate formate. Conversely, the terminal OH groups have been demonstrated to react with CO to form unidentate formate which is converted to bidentate formate (*2*). Adsorbed CO and water were not observed under the present conditions.

As already mentioned, the intermediate of WGSR (from H_2O(−OH) and CO) on

ZnO is bidentate and the intermediate of r-WGSR (from $H_2 + CO_2$) is also bidentate formate. However, the decomposition selectivity of those formates is different each other, suggesting that WGSR and r-WGSR proceed on different sites of ZnO surface, though WGSR is an equilibrium reaction with r-WGSR and they have been assumed to proceed at the same site. The active sites of WGSR involve the bridge-site and hollow-site OD which shows the peaks at 2682 and 2669 cm^{-1}, respectively, while the active sites of r-WGSR involve the hollow-site OD which shows the peak at 2602 cm^{-1}.

CONCLUSIONS

(1) Bidentate formate is produced from $H_2 + CO_2$ on a ZnO surface, similarly to the case from $-OH(H_2O) + CO$.

(2) However, the decomposition selectivity for the formate from $H_2 + CO_2$ is different from that from $-OH(H_2O) + CO$. Ca. 70% of the former formate decomposed to $H_2 + CO_2$ and 30% of them decomposed to $H_2O + CO$. On the contrary, 30% of the latter formate decomposed to $H_2 + CO_2$ and 70% of them decomposed to $-OH(H_2O) + CO$.

(3) It is suggested that WGSR and r-WGSR proceed through the bidentate formate, but at different sites.

(4) Decomposition of formate is promoted 8–10 times by the coadsorption of hydrogen, whereas it is suppressed by the coadsorption of CO_2.

(5) By the coadsorption of hydrogen, the activation energy decreases from 171 kJ mol^{-1} (in vacuum) to 138 kJ mol^{-1}.

(6) Decomposition selectivity of the formate is not changed by the coexistence of hydrogen or CO_2, which is different from the case in the presence of electron-donor molecules such as water, methanol, ammonia, and pyridine.

REFERENCES

1. Shido, T., Asakura, K., and Iwasawa, Y., *J. Catal.* **122,** 55 (1990).
2. Shido, T. and Iwasawa, Y., *J. Catal.* **129,** 353 (1991).
3. Shido, T. and Iwasawa, Y., *J. Catal.* **136,** 493 (1992).
4. Shido, T. and Iwasawa, Y., *J. Catal.*, in press.
5. Sholten, J. J. F., Mars, P., Menon, P. G., and Hardevald, R. Van, *in* "Proceedings, 3rd International Congress on Catalysis, Amsterdam, 1964," Vol. 2, p 881. Wiley, New York, 1965.
6. Ueno, A., Onishi, T., and Tamaru, K., *Trans. Faraday Soc.* **66,** 756 (1970).
7. Little, L. H., "Infrared Spectra of Adsorbed Species." Academic Press, London, 1966.
8. Saussey, J., Lavalley, J. C., Bovet, C., *J. Chem. Soc. Faraday Trans. 1,* **78,** 1457 (1982).
9. Nakamoto, K., "Infrared and Raman Spectra of Inorganic and Coordination Compounds," 3rd ed. Wiley–Interscience, New York, 1987.
10. Eischens, R. P., Pliskin, W. A., and Low, M. J. D., *J. Catal.* **1,** 180 (1962).
11. Naito, S., Shimizu, H., Hagiwara, E., Onishi, T., Tamaru, K., *Trans. Faraday Soc.* **67,** 1519 (1971).
12. Tsyganenko, A. A., and Filimonov, V. N., *J. Mol. Struct.* **19,** 579 (1973).
13. Boehm, H. P., and Knözinger, H., *in* "Catalysis" (J. R. Anderson and M. Boudart, Eds.), Vol. 4, p. 39. Springer, Berlin, 1983.
14. Dent, A. L., and Kokes, R. J., *J. Phys. Chem.* **63,** 3781 (1969).
15. Shido, T., Asakura, K., and Iwasawa, Y., *J. Chem. Soc. Faraday Trans. 1* **85,** 441 (1989).